Desalination and Water Treatment
www.deswater.com
doi: 10.1080/19443994.2015.1076352

57 (2016) 16111–16118
July

Taylor & Francis
Taylor & Francis Group

Ag-TiO$_2$ nanoparticles for photocatalytic degradation of lomefloxacin

Raviraj M. Kulkarni[a,*], Ramesh S. Malladi[a], Manjunath S. Hanagadakar[a], Mrityunjay R. Doddamani[b], Udaya K. Bhat[c]

[a]*Department of Chemistry, KLS Gogte Institute of Technology, (Affiliated to Visvesvaraya Technological University), Belagavi 590008, Karnataka, India, Tel. +91 8312498511; Fax: +91 8312441909; emails: ravirajmk@git.edu (R.M. Kulkarni), rameshmalladi7@gmail.com (R.S. Malladi), manju.hanagadakar@gmail.com (M.S. Hanagadakar)*
[b]*Mechanical Engineering, National Institute of Technology Karnataka, Surathkal, India, Tel. +91 8242473678; email: Mrd1978@rediffmail.com*
[c]*Metallurgical and Materials Engineering, National Institute of Technology Karnataka, Surathkal, India, Tel. +91 8242474000; email: udayabhatk@gmail.com*

Received 5 January 2015; Accepted 21 July 2015

ABSTRACT

The photocatalytic activity of silver-doped TiO$_2$ (Ag-TiO$_2$) nanoparticles was studied by photocatalytic degradation of lomefloxacin (LMF) using a photoreactor with a mercury lamp (PHILIPS, TUV 8 W T5, E_{max} = 254 nm). The 1 and 2% silver-doped TiO$_2$ nanoparticles were synthesized by liquid impregnation (LI) method. The resulting nanoparticles were characterized by surface analytical methods such as X-ray diffraction (XRD), scanning electron microscope (SEM), energy dispersive X-ray analysis and transmission electron microscope (TEM). The study shows 2% Ag-TiO$_2$ nanoparticles exhibited better results (95% degradation) in 1 h for the degradation of lomeofloxacin compared to 1% Ag-TiO$_2$ and pure TiO$_2$. XRD analysis indicated that the crystallite size of TiO$_2$ was 17.00 nm, while the crystallite size of 1% Ag-TiO$_2$ and 2% Ag-TiO$_2$ was 13.07 to 14.17 nm. TEM images show the particle size of Ag-TiO$_2$ nanoparticles were in the range 40–45 nm in length and 10–15 nm in breadth. Pseudo-first-order rate constants were found to decrease with increase in pH. The effect of UV intensity, catalyst dosage and initial concentration of LMF on the degradation rate were also studied and elaborately discussed.

Keywords: Titanium dioxide; Liquid impregnation; Photocatalysis; Lomeofloxacin; AOP

1. Introduction

Advanced oxidation processes (AOPs) are techniques designed for the degradation of harmful organic contaminants which are resistant to conventional and biological treatment methods. AOPs depend on the generation of highly reactive radical species such as OH$^\cdot$ that decompose a number of organic contaminants without being selective [1–3] using chemical or light energy. The AOPs normally involve a semiconductor photocatalyst activated by UV or visible light resulting in partial or complete mineralization of the organic molecules [4,5].

There are several studies related to the use of TiO$_2$ in the photomineralization of pharmaceutical compounds [6,7].

Titanium dioxide (TiO$_2$), a metal oxide semiconductor has been found to be one of the most

---

*Corresponding author.

effective photocatalysts due to its chemical structure, biocompatibility, high efficiency low cost and optical and electrical properties [8,9]. TiO_2 has a band gap of 3.2 eV that allows UV light to excite the valance electrons into the conduction band leaving holes in the valance band [10]. The high rate of electron–hole recombination in TiO_2, however, limits the efficiency of the photocatalyst which can be prevented, to some extent, by doping with noble metals such as silver, gold, platinum [11]. The most important advantage of the doping of silver on TiO_2 is improving the charge separation efficiency of the TiO_2. Moreover, the antibacterial action of silver, particularly in the colloidal form, is also well reported [12].

Lomefloxacin (LMF) is an antibacterial agent which belongs to the fluoroquinolone family, it is used to treat various bacterial infections, such as urinary tract, bronchitis etc. Now-a-days, antibacterial agents have been used in large amount for last few decades; these agents enter in to the environment through domestic sewage due to partial metabolism in the human body [13]. The chemical structure of LMF is given in Fig. 1.

However, no significant efforts have been made to investigate the detailed degradation kinetics, which is essential for the application point of view. Hence, we have carried out a detailed study on the photocatalytic degradation of LMF by Ag-TiO_2 nanoparticles in aqueous medium examining various reaction parameters such as pH, substrate and catalyst concentration, intensity of UV light. In the present work, TiO_2 nanoparticles were doped with silver using liquid impregnation (LI) technique. These nanoparticles were characterized by the techniques such as X-ray diffraction (XRD), scanning electron microscope (SEM), energy dispersive X-ray analysis (EDX) and transmission electron microscope (TEM).

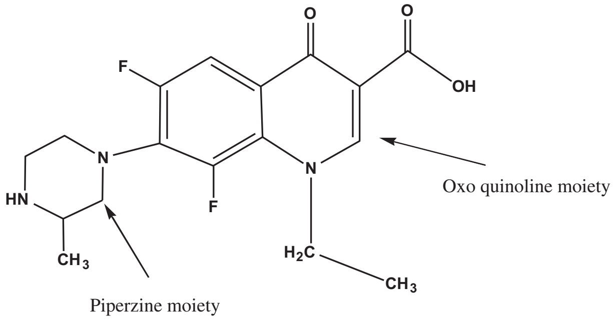

Fig. 1. Chemical structure of lomefloxacin.

2. Experimental

2.1. Materials and methods

A stock solution of LMF (Gift sample from Dr Reddy's laboratories) was prepared by dissolving appropriate amount of sample in double distilled water. The TiO_2 sample was purchased from Sisco Research Pvt. Ltd, Mumbai 93. India (TiO_2-Anatase). $AgNO_3$ purchased from HIMEDIA. The analytical grade chemicals were used to prepare acetate (pH 4–5), phosphate (pH 6.0–8.5) and borate (pH 9) buffers.

2.1.1. Instruments used

(1) For kinetic measurements, a CARY 50 Bio UV–vis spectrophotometer (Varian BV, The Netherlands) with temperature controller and HPLC system (Agilent 1100 series, USA) were used.
(2) For degradation study, a photoreactor with mercury lamp (PHILIPS, TUV 8 W T5, E_{max} = 254 nm) was used. The typical light intensity illuminated on the surface of reaction mixture was 4 mW/cm^2.
(3) For UV light intensity measurements, an optical power metre (Newport 2936-C) and for pH measurements, Elico pH metre models LI 120 were used.
(4) For characterization of nanoparticles, a Siemens X-ray diffractometer (Cu source) (XRD) AXS D5005 was used to identify the particle size of the doped TiO_2. The surface morphologies were examined using a scanning electron microscope (SEM) JEOL JSM 6360.
(5) The topography and particle size of Ag-TiO_2 was measured using JEOL JEM-2010 TEM.

2.2. Photo catalyst preparation

2.2.1. LI method

500 mg of TiO_2 was added to 100 ml deionized water in a 500 ml Pyrex beaker. For silver doping 1 and 2% (molar ratio) of $AgNO_3$ was also added to the suspension. The resulting slurry was thoroughly mixed by vigorous stirring and allowed to settle at room temperature overnight. The liquid so obtained was dried in an oven at 100˚C for 12 h to get rid of any remaining moisture. The solid material resulting from this step was calcined at 500˚C for 3 h in a muffle furnace. This resulted in fine particles of Ag-TiO_2 nanoparticles [14,15].

2.3. The photocatalysis process

To investigate the photocatalytic degradation, a known concentration of LMF solution and buffer was taken in a Pyrex beaker. A dose of 100 mg/l 2% Ag-TiO_2 nanoparticles was added. Then, it was transferred in to the photoreactor and then kept under 8 W UV lamps (Philips) with a wavelength peak at 254 nm and of 4 mW/cm^2 intensity with continuous stirring. After every 15 min interval, the solution was taken out and centrifuged at 2,000 rpm for 5 min. The degradation of centrifuged solution was measured at 287 nm (ε = 27,209 L M^{-1} cm^{-1}) using visible spectrophotometer (a CARY 50 Bio UV–vis spectrophotometer (Varian BV, The Netherlands)) and the degree of mineralization was studied.

3. Results and discussion

3.1. Comparison of different photocatalysts

The rate of photo catalytic degradation of LMF with UV, UV/TiO_2, UV/(1%) Ag-TiO_2 and UV/(2%) Ag-TiO_2 was studied. It is observed that the degradation effect of LMF treatment with UV/Ag-TiO_2 was more efficient than other two treatments namely UV and UV/TiO_2.

Effect of silver doping on anatase TiO_2 was studied by changing the percentage of silver from 1 to 2% (mole ratio) an increase in the content of silver leads to decrease in the particle size and increase in the photocatalytic activity as shown in Fig. 2. Smaller particle size increases surface area and higher content silver may also favour separating charge carriers efficiently, inhibiting the recombination of electron–hole pairs, and thus increasing the photocatalytic activity [16]. The photodegradation rate was highest with 2% Ag-TiO_2; hence, further studies were carried out with 2% Ag-TiO_2.

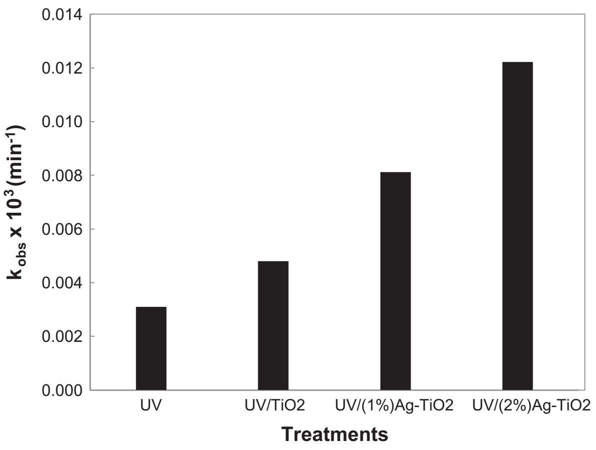

Fig. 2. Rate constants for the photocatalytic degradation of LMF by various treatments.

3.2. Characterization of TiO_2 and Ag-TiO_2

The crystal phase of prepared nanoparticles was identified using X-ray diffractometer as shown in Fig. 3. The data indicates that the major phase of all the prepared nanoparticles is anatase. The average crystalline size of prepared nanoparticles was determined from the broadening of the anatase main intense peak (1 0 1), using Scherrer equation (1), which is shown in Table 1. Crystallite size of pure TiO_2 is of 17.00 nm, while the crystallite size of Ag-TiO_2 1% is 14.17 nm, Ag-TiO_2 2% 13.07. Our results are in accordance with earlier report [7], where Ag-TiO_2 nanoparticles dimensions were reported in between 15 and 37 nm.

$$D = \frac{0.94\lambda}{\beta_{1/2} \cos \theta} \tag{1}$$

where D is the average crystalline diameter, λ is the wavelength in angstrom, β is the line width at half-maximum and θ is the Bragg angle.

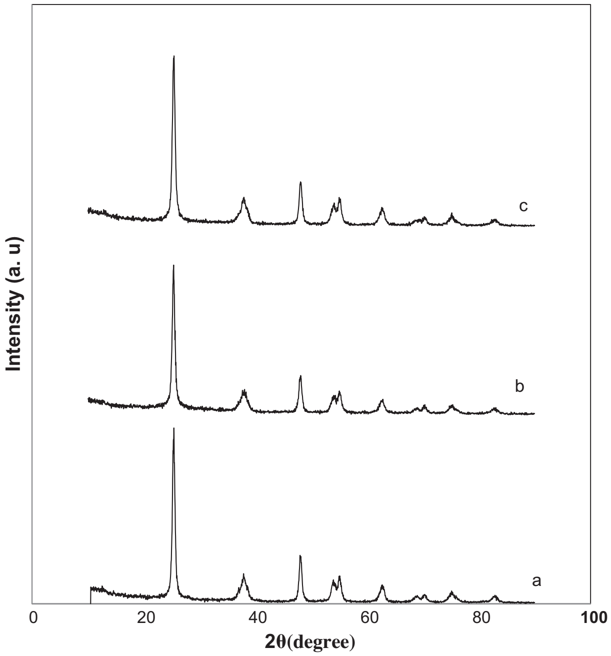

Fig. 3. XRD patterns of (a) undoped TiO_2, (b) 1% and (c) 2% Ag-TiO_2.

Table 1
Crystal size of undoped and Ag doped TiO_2 nanoparticles from Scherrer equation

Sl. no.	Particles	Particle size (nm)
1	Un doped TiO_2	17.00
2	1% Ag-TiO_2	14.17
3	2% Ag-TiO_2	13.07

3.3. Surface morphology study

3.3.1. Scanning electron microscope

The SEM images have been used to characterize the size, shape and morphologies of formed nanoparticle clusters. It shows the non-uniform aggregates of the Ag-TiO_2 nanoparticles, which results in a high surface area. (Fig. 4(a)–(c)) represents the SEM images of the undoped and prepared Ag-TiO_2 nanoparticles [12].

3.3.2. Transmission electron microscope

TEM images show the heterogeneously dispersed aggregates of Ag-TiO_2 nanoparticles having cylindrical shape crystalline structures which can be clearly observed in (Fig. 5(a) and (b)). Dispersion of small dark spots seen were presumed as Ag particles on TiO_2 nanoparticles with a particle size of approximately 10–15 nm in breadth and 40–45 nm in length. It is revealed that the crystallite size of the synthesized nanoparticles is close to that of TiO_2 nanoparticles obtained from XRD values.

3.3.3. Electron diffraction X-ray spectroscopy

EDX examination provides information on chemical composition of samples. Fig. 6(a) and (b) shows that the prepared sample is mainly composed of Ti and O with small amount of Ag that increases with increase number of loading. Ag L peak was found, but peak of Ag K cannot be detected because low electron accelerating voltage was applied [17].

3.4. Effect of photocatalyst loading

To study the effect of catalyst loading, different amounts of catalyst were used from 50 to 250 mg/l while keeping [LMF] and pH 4 constant. It has been observed that initially the rate of photo degradation increases up to 100 mg/l, beyond 100 mg/l the rate of reaction almost constant (Fig. 7). This may be due to the fact that as the amount of semiconductor was increased in the initial state, the exposed surface area of the semiconductor also increases, but after this limiting value (100 mg/l) any increase in the amount of semiconductor increases the turbidity of the solution and thus blocks UV irradiation for the reaction to proceed, and therefore degradation starts decreasing [18].

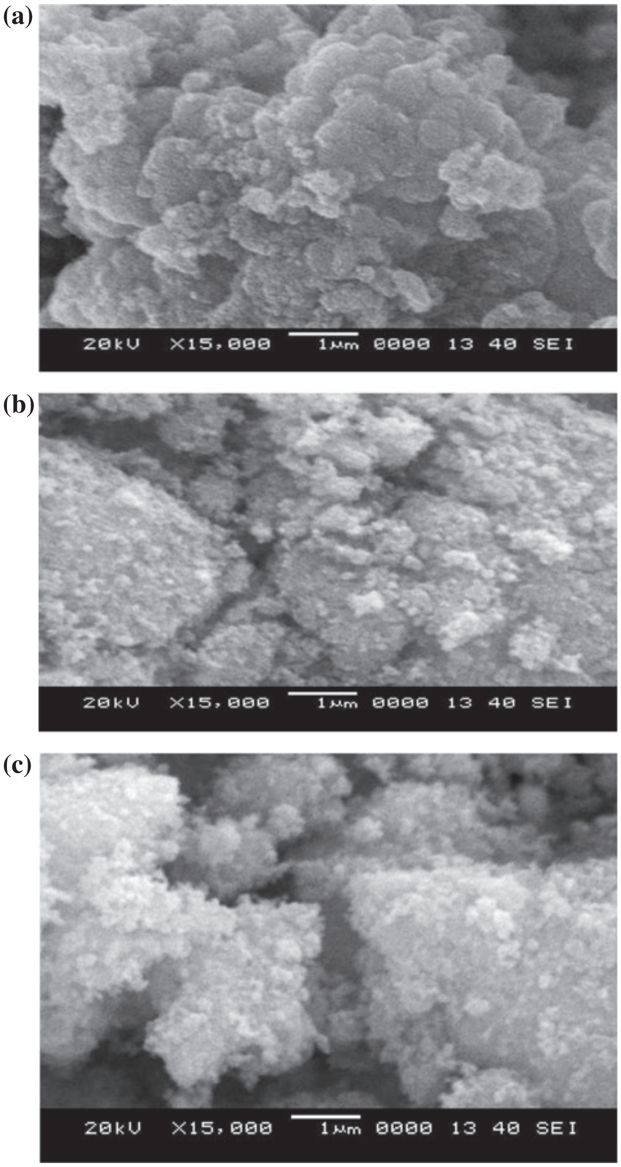

Fig. 4. SEM micrographs of (a) undoped TiO_2, (b) 1% Ag-TiO_2 and (c) 2% Ag-TiO_2.

3.5. Effect of substrate concentration

The effect of variation of LMF concentration was studied by taking different concentration of LMF from 8×10^{-5} to 28×10^{-5} mol dm^3 by keeping other condition constant. It has been observed that with the initial

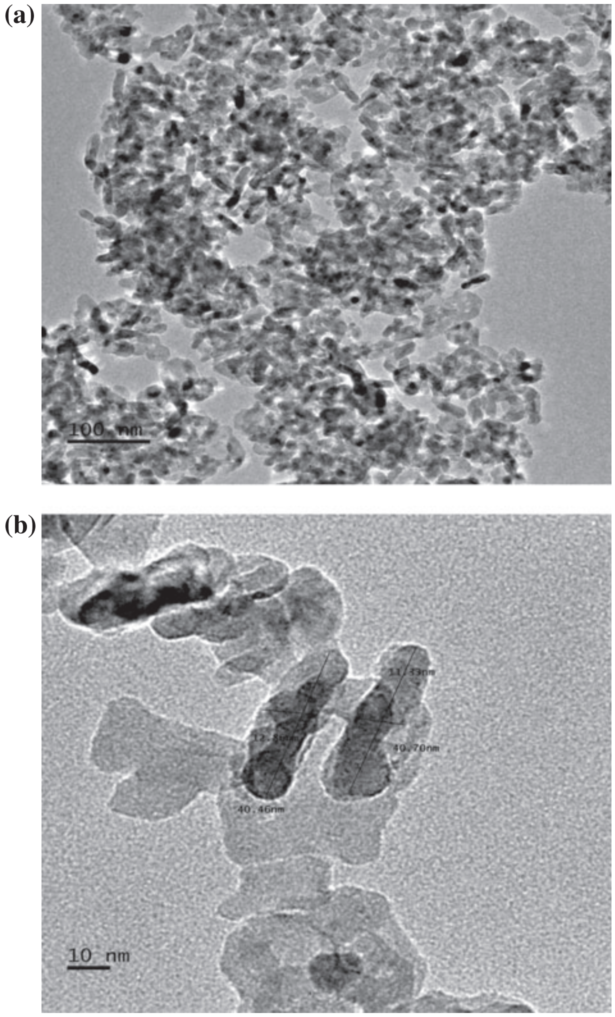

Fig. 5. TEM micrographs of 0.2% Ag/TiO_2.

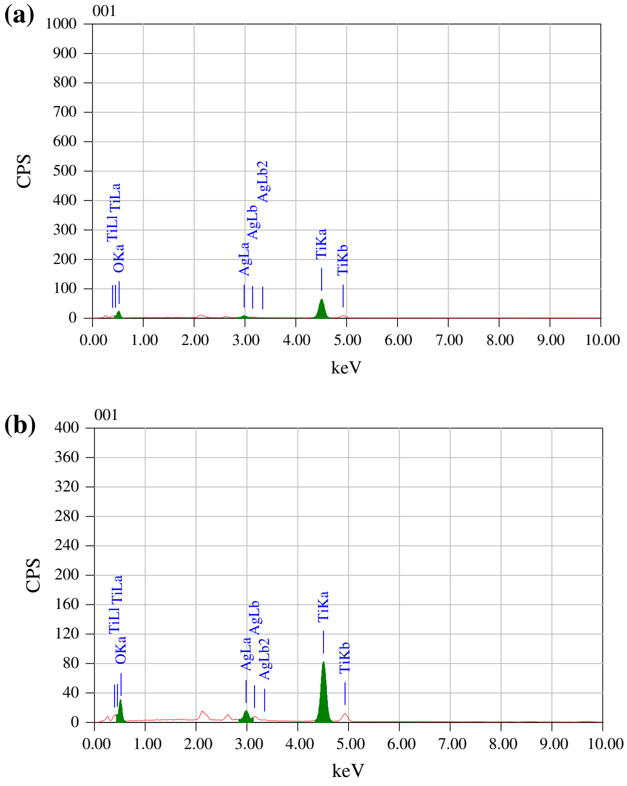

Fig. 6. (a) EDX analysis of 1% Ag-TiO_2 and (b) EDX analysis of 2% Ag-TiO_2.

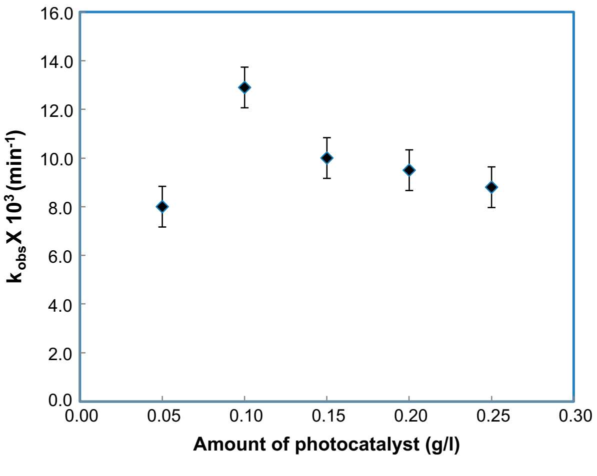

Fig. 7. Effect of different amounts of photocatalyst [LMF] = 20 × 10^{-5} M, at pH 4.

increase in the concentration of LMF, the rate of photocatalytic degradation increases, reaching maximum value [LMF] = 20 × 10^{-5} mol dm^3; further increase in concentration resulted in decrease in the rate of photocatalytic degradation as shown in Fig. 8. It may be due to the fact that, as the concentration of the drug increased, more number of drug molecules are excited and consequently available for degradation, and hence the rate of degradation increases. But at concentration above 20 × 10^{-5} mol dm^3, the drug itself acts as a filter for the incident light. This reduces the formation of OH^- ions, due to which, the rate of photocatalytic degradation decreases [19].

3.6. Effect of pH

The pH normally influences the adsorption capacity of the adsorbent in aqueous medium by altering the surface properties of adsorbent. The effect of pH on the rate of photo degradation of LMF was studied by varying the pH from 4 to 8, while keeping other conditions constant. The rate of photocatalytic degradation of LMF was slightly higher in the pH

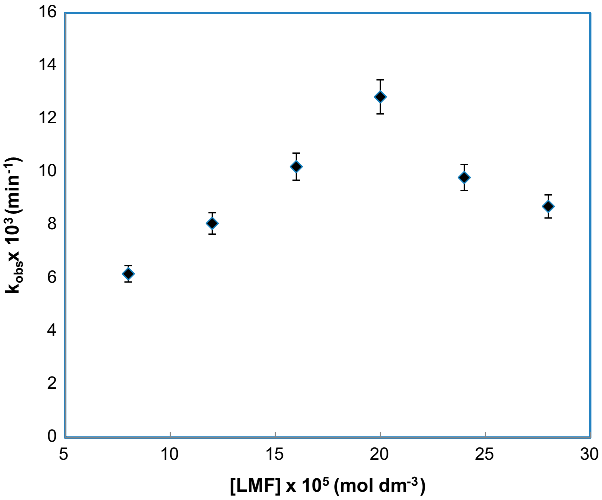

Fig. 8. Effect of variation of [LMF] on photocatalytic rate constants of photocatalytic process with 2% Ag-TiO_2 at 25˚C, [Ag-TiO_2] = 100 mg/l, at pH 4.

range 4–5 and slightly lower in the pH range 7–8 as shown in Fig. 9. This behaviour may be explained on the basis that an increase in the rate of photocatalytic degradation may be due to the increased availability of OH^- ions at acidic pH value. OH^- ions will generate more hydroxyl radicals (·OH) by combining with holes, which are considered responsible for the photocatalytic degradation. The adsorption on Ag-TiO_2 primarily depends on its surface properties and surface reactivity largely related to surface hydroxyl groups. It is evident from Table 2 that the adsorption capacity decreases with increase in the pH from 4 to 8. The LMF contains >NH and carboxyl functional groups in its molecular structure. This enables LMF to react with the H^+ and OH^- in solution to form three different LMF species viz., $LMFH^+$ (cation), LMF° (neutral) and LMF^- (anion). The pK_a values of LMF were computed by using Chem axon calculator and they were found to be pK_{a1} (5.64) and pK_{a2} (8.7) [20]. The proportion of LMF in different forms can be calculated from the pK_a values of LMF. The speciation pattern of LMF at different pH is shown in Fig. 10. LMF forms about 98% $LMFH^+$ at pH 4 by combining with H^+ ions from the solution, which favours the LMF adsorption on the negatively charged surface of Ag-TiO_2 photocatalyst. The propotion of $LMFH^+$ decreases to 81% at pH 5, reduces to 30% at pH 6 and further reduces to 4% (negligible) at pH 7. LMF neutral species dominates in the pH range 6–8. With the proportional decrease in the concentration of $LMFH^+$ and proportional increase in the concentration of LMF neutral, the adsorption capacity of LMF on Ag-TiO_2 decreases. The adsorption of $LMFH^+$ is due to the combination of cation with negatively charged surface of Ag-TiO_2, whereas the adsorption of LMF neutral is due to weak Van der Waals forces of attraction. This observation is in line with the earlier report [21].

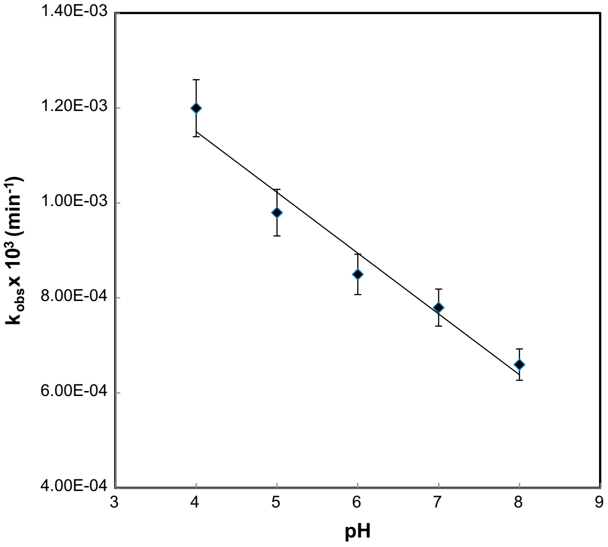

Fig. 9. Effect of pH on the rate constant of photo catalytic degradation of LMF with 2% Ag-TiO_2 at 25˚C, [Ag-TiO_2] = 100 mg/l, [LMF] = 20 × 10^{-5} M.

3.7. Effect of UV lamp distance

To examine the effects of UV light intensity on the degradation of lomeofloxin was studied by varying the distance of UV lamp from the target. The results are reported in Fig. 11. It is seen that an increase in light intensity increase the rate of photocatalytic degradation, and it is due to the fact that as the intensity increases the more number of Ag-TiO_2 nanoparticles excite to generate more electron hole pairs. The holes decompose the lomeofloxin molecules adsorbed on the surface of Ag-TiO_2 particles and oxidize it to water resulting in their efficient degradation [22].

3.8. Mechanism of photocatalytic degradation

On the basis of the experimental data the following tentative mechanism may be given for photocatalytic degradation of LMF.

$$^1LMF_0 \xrightarrow{h\upsilon} {}^1LMF_1$$

$$^1LMF_1 \xrightarrow{ISC} {}^3LMF_1$$

Table 2
Adsorption capacity at different pH (Langmuir isotherm)

Sl. no.	pH	Adsorption capacity (Langmuir isotherm) (mol/g)
1	4	0.00110
2	5	0.00091
3	6	0.00085
4	7	0.00072
5	8	0.00062

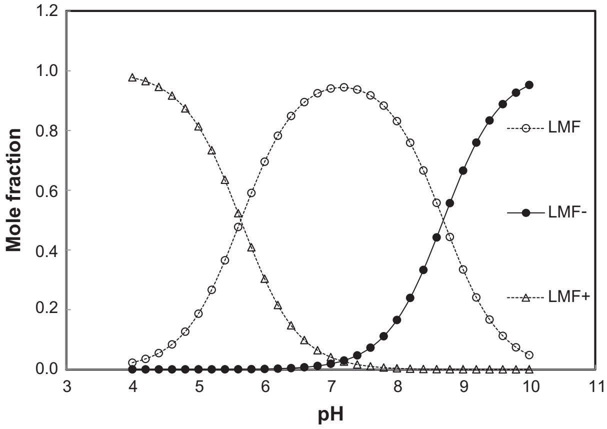

Fig. 10. Speciation of LMF at different pH.

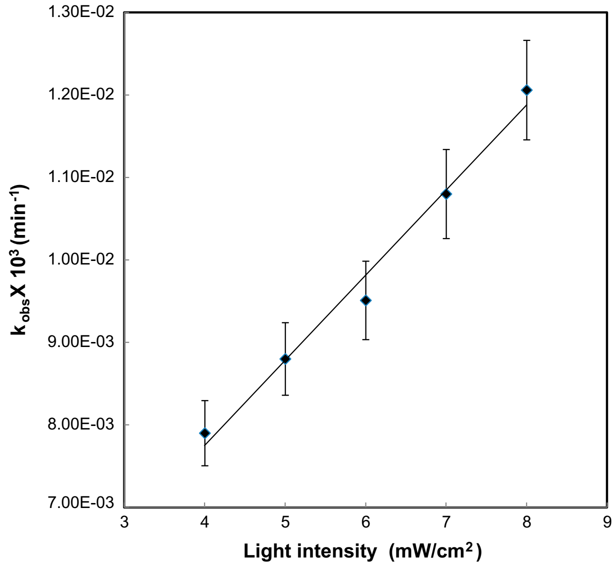

Fig. 11. LMF degradation under different UV intensities LMF with 2% Ag-TiO_2 at 25˚C, [Ag-TiO_2] = 100 mg l^{-1}, [LMF] = 20 × 10^{-5} M, at pH 4.

$$^3LMF_1 + Ag\text{-}TiO_2 \longrightarrow LMF^+ + Ag\text{-}TiO_2(e^-)$$

$$Ag\text{-}TiO_2(e^-) + O_2 \longrightarrow Ag\text{-}TiO_2 + O_2^{-\cdot}$$

$$LMF^+ + OH^- \longrightarrow LMF + OH^\cdot$$

$$LMF + OH^\cdot \longrightarrow Product$$

When the LMF solution is exposed to UV light, in the presence of Ag-TiO_2, initially LMF molecules are excited to first singlet state ($^1LMF_1$). Then these excited molecules are moved to the triplet state through inter system crossing (ISC). The triplet drug ($^3LMF_1$) may provide its electron to the photocatalyst and become positively charged. The dissolved oxygen of the solution will pull an electron from the conduction band of the photocatalyst, thus generating the photocatalyst. The positively charged molecules of the drug (LMF) will immediately reacts with ^-OH ions to form $OH^\cdot$ radicals, which will convert the drug molecules in to products.

In undoped TiO_2, molecular oxygen is the only one electron trapping entity, whereas in Ag-TiO_2, two other electron trapping entities are set up, viz., Ag^+ ions and Ag^0. Since the Fermi level of TiO_2 is higher, hence electrons will move from TiO_2 nanoparticles to the metallic silver nanoparticles resulting in a space charge between Ag and TiO_2. The electric field finally force the electrons to the interfacial space of the TiO_2 nanoparticles. Here, silver particles act as electron traps [23]. This leads to an increase in the charge separation efficiency and slows down electron–hole recombination. Silver metal on the catalyst surface improves the quantum yields by increasing the removal and the transfer of electrons from catalyst to molecular oxygen [24]. Therefore, molecular oxygen can trap photogenerated electrons to form superoxide radicals and consequently enhance the oxidation of LMF.

4. Conclusion

1 and 2% silver doped TiO_2 nanoparticles were synthesized successfully by LI method. The XRD patterns of synthesized Ag-TiO_2 nanoparticles indicate anatase crystal structure. The EDX analysis and TEM topograph show the doping of silver in TiO_2. In acidic environment at pH 4, the prepared Ag-TiO_2 nanoparticles (17.00–13.07 nm) exhibit good potential for the photocatalytic degradation of LMF. It is evident from the results that over 95% degradation of LMF could be achieved in 1 h using 2% Ag-TiO_2 photocatalyst.

References

[1] T. Kudo, Y. Nakamura, A. Ruike, The design of highly active rectangular column structured titanium oxide photocatalysts and their application in purification systems, J. Catal. Today 122 (2003) 14–19.

[2] G. Zayani, L. Bousselmi, F. Mhenni, A. Ghrabi, Solar photocatalytic degradation of commercial textile azo dyes: Performance of pilot plant scale thin film fixed-bed reactor, Desalination 246 (2009) 344–352.

[3] U.I. Gaya, A.H. Abdullah, Heterogeneous photocatalytic degradation of organic contaminants over titanium dioxide: A review of fundamentals, progress and problems, J. Photochem. Photobiol. C 9(1) (2008) 1–12.

[4] C. Guillard, J. Disdier, J.M. Herrmann, C. Lehaut, T. Chopin, S. Malato, J. Blanco, Comparison of various titania samples of industrial origin in the solar photocatalytic detoxification of water containing 4-chlorophenol, Catal. Today 54 (1999) 217–228.

[5] P. Bansal, N. Bhullar, D. Sud, Studies on photodegradation of malachite green using TiO_2/ZnO photocatalyst. Desalin. Water Treat. 12(1–3) (2009) 108–113.

[6] A. Jodat, A. Jodat, Photocatalytic degradation of chloramphenicol and tartrazine using Ag/TiO_2 nanoparticles, Desalin. Water Treat. 52(13–15) (2014) 2668–2677.

[7] A. Verma, I.D. Chhikara Photocatalytic treatment of pharmaceutical industry wastewater over TiO_2 using immersion well reactor: Synergistic effect coupling with ultrasound, Desalin. Water Treat. 52(34–36) (2014) 6591–6597.

[8] Y. Yang, X.J. Li, J.T. Chen, L.Y. Wang, Effect of doping mode on the photocatalytic activities of Mo/TiO_2, J. Photochem. Photobiol., A 163(3) (2004) 517–522.

[9] K.V. Baiju, C.P. Sibu, K. Rajesh, P.K. Pillai, P. Mukundan, K.G.K. Warrier, W. Wunderlich, An aqueous sol–gel route to synthesize nanosized lanthana-doped titania having an increased anatase phase stability for photocatalytic application, Mater. Chem. Phys. 90 (2005) 123–127.

[10] C. Kormann, D.W. Bahnemann, M.R. Hoffmann, Preparation and characterization of quantum-size titanium dioxide, J. Phys. Chem. 92 (1988) 5196–5201.

[11] M.S. Lee, S.S. Hong, M. Mohseni, Synthesis of photocatalytic nanosized TiO_2–Ag particles with sol-gel method using reduction agent, J. Mol. Catal. A 242 (2005) 135–140.

[12] D. Guin, S.V. Manorama, J.N.L. Latha, S. Singh, Photoreduction of Silver on Bare and Colloidal TiO_2 nanoparticles/nanotubes: Synthesis, characterization, and tested for antibacterial outcome, J. Phys. Chem. C 111 (2007) 13393–13397.

[13] B. Halling-Sørensen, S.N. Nielsen, P.F. Lanzky, F. Ingerslev, H.C. Holten Lützhøft, S.E. Jørgensen, Occurrence, fate and effects of pharmaceutical substances in the environment—A review, Chemosphere 36(2) (1998) 357–393.

[14] M.A. Behnajady, N. Modirshahla, M. Shokri, B. Rad, Enhancement of photocatalytic activity of TiO_2 nano particles by silver doping: Photodeposition versus liquid impregnation methods, Global NEST J. 10(1) (2008) 1–7.

[15] H. Ilyas, I.A. Qazi, W. Asgar, M.A. Awan, Z. Khan, Photocatalytic degradation of nitro and chlorophenols using doped and undoped titanium dioxide nanoparticles, J. Nanomater. 2011 (2011) 1–8.

[16] U.S. Ozkan, M.W. Kumthekar, G. Karakas, Characterization and temperature-programmed studies over Pd/TiO_2 catalysts for NO reduction with methane, Catal. Today 40(1) (1998) 3–14.

[17] K. Wetchakun, S. Phanichphant, Effect of Ru on photocatalytic activity of TiO_2 nanoparticles, J. Microsc. Soc. Thailand 22 (2008) 11–14.

[18] J. Sun, L. Qiao, S. Sun, G. Wang, Photocatalytic degradation of Orange G on nitrogen-doped TiO_2 catalysts under visible light and sunlight irradiation, J. Hazard. Mater. 155 (2008) 312–319.

[19] C.C. Wang, C.K. Lee, M.D. Lyu, L.C. Juang, Photocatalytic degradation of C.I. Basic Violet using TiO_2 catalysts supported by Y. Zeolite an investigation of the effects of operational parameters, Dyes Pigm. 76 (2008) 312–319.

[20] Marvin 5.10.1, 2012, ChemAxon. Available from: <http://www.chemaxon.com>.

[21] I.T. Horvath, Heterogeneous photocatalytic degradation of organic contaminants over titanium dioxide: A review of fundamentals, progress and problems, J. Encycl. Catal. 5 (2003) 577–599.

[22] Z. Guo, R. Ma, G. Li, Degradation of phenol by nanomaterial TiO_2 in wastewater, Chem. Eng. J. 119 (2006) 55–59.

[23] C. He, Y. Yu, X. Hu, A. Larbot, Influence of silver doping on the photocatalytic activity of titania films, Appl. Surf. Sci. 200 (2002) 239–247.

[24] H. Gerischer, A. Heller, Photocatalytic oxidation of organic molecules at TiO_2 particles by sunlight in aerated water, J. Electrochem. Soc. 139 (1992) 113–118.